

ARTICLE

A deep learning long short-term memory model for reduction of inter-carrier interference in orthogonal frequency division multiplexing systems

Sailakshmi Kumari Narava*^{ORCID}, and Kavi Priya Periasami^{ORCID}

Department of Electronics and Communication Engineering, School of Computing, Sathyabama Institute of Science and Technology, Chennai, Tamil Nadu, India

(This article belongs to the *Special Issue: Emerging Systematic Innovation Tools and Techniques for Smart Health and Education*)

Abstract

Wireless network performance depends extensively on the carrier interference. Inter-carrier interference (ICI) can be caused by several factors, including carrier frequency offsets, Doppler spread due to channel time variation, and sampling frequency offsets, which degrade the performance of an orthogonal frequency division multiplexing (OFDM) system. Hence, reducing ICI is a major task in communication systems. The lower the ICI, the higher the performance of the OFDM system. Moreover, the application of deep learning has demonstrated significant improvements in communication reliability and reduced the computational complexity of 5G and subsequent networks. Deep learning combined with ICI self-cancellation techniques yields promising results. In this paper, a hybrid framework leveraging mirror-based techniques is developed to enhance data robustness and mitigate interference while using deep learning models for adaptive, real-time ICI prediction and suppression. We incorporated multiple symbol rates and multi-carrier vector transmission at the physical layer to improve signal resilience against channel imperfections. These techniques were used in conjunction with deep learning models such as long short-term memory (LSTM) to predict ICI patterns and dynamically adjust mirror-based symbol-repetition parameters to optimize signal quality. The LSTM was incorporated with an attention mechanism. Improved interference cancellation was observed through the combined strength of symbol repetition and adaptive neural network-based interference prediction. The performance of the proposed work was evaluated using two modulation techniques: quadrature phase-shift keying and binary phase-shift keying. The results for bit error rate and carrier-to-interference ratio were best with ICI self-cancellation combined with LSTM. In summary, the proposed approach improves OFDM system performance by eliminating ICI and enhancing signal quality.

Keywords: Orthogonal frequency division multiplexing system; Inter-carrier interface; Self-inter-carrier interface cancellation; Long short-term memory; Bit error rate; Modulation techniques

***Corresponding author:**
Sailakshmi Kumari Narava
(sailaxmi2@gmail.com)

Citation: Narava, S. K., & Periasami, K. P. (2026). A deep learning long short-term memory model for reduction of inter-carrier interference in orthogonal frequency division multiplexing systems. *Int J Systematic Innovation*, 10(3): 026020002.

[https://doi.org/10.6977/IJoSI.202606_10\(3\).0003](https://doi.org/10.6977/IJoSI.202606_10(3).0003)

Received: January 7, 2026

Revised: March 26, 2026

Accepted: April 10, 2026

Published online: June 10, 2026

Copyright: © 2026 Author(s). This is an Open-Access article distributed under the terms of the Creative Commons Attribution License, permitting distribution, and reproduction in any medium, provided the original work is properly cited.

Publisher's Note: AccScience Publishing remains neutral with regard to jurisdictional claims in published maps and institutional affiliations.

1. Introduction

Orthogonal frequency division multiplexing (OFDM) is among the most popular methods in wireless communication systems today because it is highly spectral-efficient, resistant to multipath fading, and capable of supporting high data rates. It is also used to transmit multiple bit streams in parallel, as the available bandwidth is partitioned into a series of orthogonal subcarriers, making it efficient in spectrum use. Consequently, the use of OFDM has become a central technology across a range of communication standards, such as wireless local area networks (WLAN), digital video broadcasting (DVB), and fourth-generation (4G) and fifth-generation (5G) mobile communication networks. Although these benefits exist, synchronization errors and channel malfunctions can severely affect the performance of OFDM systems and compromise communication reliability (Li *et al.*, 2020).

Inter-carrier interference (ICI) is one of the biggest problems of OFDM systems. It occurs when the orthogonality between subcarriers is disrupted either by carrier frequency offset, the Doppler shift of the moving user, or oscillator mismatch between the sender and receiver. ICI causes energy leakage between subcarriers, leading to interference and poor signal quality. As a result, the bit error rate (BER) increases, and the overall system performance is affected. Therefore, it is necessary to develop efficient methods to reduce ICI and ensure stable, efficient communication in OFDM-based systems (Mthethwa & Xu, 2020).

The literature offers several strategies to address the ICI problem. Conventional methods include frequency-domain equalization, self-cancellation methods, coding-based methods, and pilot-assisted estimation. The most frequently employed mechanisms are mirror symbol repetition (MSR) and multi-carrier vector transmission (MCVT) because they minimize interference by exploiting adjacent subcarrier correlations. MSR enhances the interference cancellation by sending mirrored symbols over the adjacent sub-carriers, while MCVT treats the subcarrier groups as vectors to identify the inter-carrier mirror relationships. In dynamic wireless environments where the interference pattern is highly nonlinear and time-varying, the effectiveness of these methods can be reduced, though they still offer noticeable improvements.

In recent years, deep learning has become a powerful tool in solving complex problems in wireless communications. Deep learning models can also learn nonlinear relationships directly from data and have been applied to tasks such as channel estimation, signal detection, interference mitigation, and resource allocation.

Particularly, the family of recurrent neural networks, including long short-term memory (LSTM) networks, is well-suited to sequential and time-dependent data. Long-term dependencies in signal sequences are also captured by LSTM networks, making them highly appropriate in predicting interference patterns in communication systems. With these capabilities, deep learning-based methods might outperform traditional signal processing methods in complex communication settings.

This paper is inspired by these benefits and proposes a deep learning-based architecture that combines the MSR and MCVT with an LSTM network to achieve effective ICI mitigation in OFDM systems. The proposed model uses an LSTM to capture temporal dependencies in the received OFDM signal and precisely approximate the interference components. This model will combine the advantages of MSR and MCVT with the learning ability of LSTM to maximize interference cancellation and signal recovery.

Bazzi *et al.* (2015) proposed a rigorous model of the mechanics of OFDM signal modeling in a rich multipath environment, in terms of a sum of scaled and delayed components, upon which the mechanism of interference in such systems is understood.

Another pre-processing method adopted in this study was spatio-frequency smoothing of the coherent multipath signal. This approach is especially applicable to our framework because it emphasizes signal conditioning before ICI mitigation.

Moreover, recent progress has highlighted deep learning-based parameter estimation for OFDM radar systems. Its use of convolutional neural networks (CNNs) to directly extract features from signal representations strongly supports the feasibility of our real-time ICI prediction method.

In addition, we proposed a mutual information-based pilot design for integrated sensing and communication systems. Bazzi *et al.* (2015) provided theoretical evidence for the effectiveness of pilot-assisted channel state information estimation in our framework. Furthermore, its focus on waveform and sequence design for next-generation (6G) systems, particularly subcarrier optimization and peak-to-average power ratio reduction, aligns closely with our use of pilot structures and mirror-based techniques to enhance robustness and system performance.

The primary findings of this work include the following:

- A new MSR-MCVT-LSTM framework is proposed to minimize ICI in OFDM systems.
- The mathematical modeling of the OFDM signal, the interference components, and the inter-interference

prediction using LSTM is presented.

- Deep learning is used to predict and reduce ICI by leveraging temporal dependencies in the received signal.
- A large number of simulations are performed to analyze the performance of the proposed method across various signal-to-noise ratios (SNRs).
- The proposed advancement offers a better carrier-to-interference ratio (CIR) and a lower BER than traditional methods.

The rest of the paper is structured as follows. Section 2 provides a review of the relevant work on ICI mitigation techniques and deep learning-based communication models. Section 3 presents the proposed MSR–MCVT–LSTM structure and mathematical formulation. Section 4 presents the simulation setup, training details, and the performance evaluation results. Lastly, Section 5 concludes the study and provides future research directions.

2. Related work

In a variety of wireless communication applications, deep learning techniques have become a prominent and current trend. This section discusses the related use of deep learning. A few factors from different disciplines enable deep learning. The fact that deep learning-based algorithms are data-driven is an important feature that helps them overcome challenges in practical applications. Furthermore, the computational complexity of deep learning-based methods is lower, requiring fewer layers of basic operations such as matrix–vector multiplications. Furthermore, deep learning algorithms can be easily implemented using low-precision data types and highly parallelized.

Ly and Yao (2021) provided a thorough analysis of deep learning research on 5G communications. They specifically examined resource allocation, security, non-orthogonal multiple access (NOMA), massive multiple-input multiple-output (MIMO), and low-density parity-check coding. Jdid *et al.* (2021) discussed automatic modulation recognition (AMR), which is crucial to most intelligent communication systems, particularly in light of the rise of software-defined radio. In spectrum sensing for cognitive radio, AMR is an essential activity. Significant progress in deep learning applications has led to the development of new and potent tools that can address issues in this field.

After reviewing the evolution of deep learning solutions for 5G communication, Huang *et al.* (2020) proposed effective plans for 5G scenarios based on deep learning. In particular, the main concepts underlying several significant deep learning-based communication techniques were discussed, along with the prospects and

difficulties for further study. The superior performance of novel communication frameworks, such as millimeter wave (mmWave), massive MIMO, and NOMA, was examined. Krishnama Raju *et al.* (2022) used hyperparameter tuning to improve the effectiveness of deep neural networks (DNNs) for channel estimation and symbol identification in OFDM systems. In wireless communications, deep learning outperformed conventional techniques, such as minimum mean-square error (MMSE), for channel estimation and symbol identification.

Using an LSTM, Essai Ali (2020) proposed an online deep-learning-based channel-state estimator for OFDM wireless communication systems. The proposed algorithm is an estimator type that uses pilot assistance. To retrieve the transmitted data, the proposed estimator was first trained offline on simulated datasets, then deployed online using channel statistics. To enhance channel estimation from the least-squares (LS) method, Le *et al.* (2021) proposed a novel deep learning-based channel estimation architecture. While the machine learning module was general-purpose and could be used with any neural network architecture, the system model was built for an arbitrary number of transceiver antennas.

A deep learning-based method for signal identification in uplink OFDM systems over time-varying channels was proposed by Wang *et al.* (2020). To identify signals, they used a bidirectional LSTM recurrent neural network. Bai *et al.* (2026) used an LSTM-based estimate to address the current constraints. After estimating the channel, the proposed estimator uses temporal averaging to reduce noise. For channels with dual selective fading, Nair and Menon (2022) proposed a DNN-based channel equalization technique. The simulation results showed that the proposed DNN estimator outperformed the linear MMSE estimate in terms of effectiveness and robustness. Using a 5G MIMO-OFDM system, they illustrated several DNN model topologies. These patterns were specifically designed for channel estimation in the presence of frequency-selective fading. Furthermore, the efficacy of the proposed DNN estimators was evaluated by comparing them with conventional MMSE and LS estimation techniques in terms of BER as a function of channel estimation errors and SNR.

Instead of using a single large DNN to jointly detect active antennas and modulation symbols, Shamasundar and Chockalingam (2020) addressed signal detection in generalized spatial modulation using a DNN and proposed a novel modularized DNN architecture that uses small sub-DNNs to identify active antennas and complex modulation symbols. Compared with the traditional maximum likelihood detector, the proposed DNN-based

detector performs better by learning deviations from the standard model.

A highly effective machine learning-based channel estimate method for OFDM systems was presented by Mei *et al.* (2021). Online estimator training is used in this method. The suggested learning-based estimator uses a straightforward learning module. As a result, the training process is substantially faster and requires much less training data. Additionally, a method for creating training data using LS estimates was proposed to gather it while the data is being sent.

Logins *et al.* (2022) demonstrated that combining a CNN with linear equalization greatly improved its performance. Depending on the device characteristics, the ideal order of linear and nonlinear blocks was the same throughout the CNN. Visible light communication uses deep learning. A time-sequence with memory prediction was used to compensate for channel impairments in the visible light communication channel. To retrieve the original broadcast signal and learn the complex channel characteristics, Miao *et al.* (2022) proposed an effective nonlinear post-equalization that combines a DNN with LSTM. A deep learning model was used for ICI cancellation in an OFDM system, along with ICI self-cancellation techniques, and is discussed in Section 3 (Greff *et al.*, 2017).

Recent studies have demonstrated the effectiveness of deep learning models, particularly recurrent neural networks, in handling sequential and complex data patterns. For example, in a comparative study of deep learning for skin disease classification, the CNN and CNN-LSTM architectures demonstrated the advantages of combining CNNs with LSTMs to capture spatial and temporal dependencies, thereby improving classification performance (Basholli *et al.*, 2025). Similarly, Reddy *et al.* (2025) demonstrated how deep learning techniques could effectively process large-scale unstructured data to generate meaningful insights. In the context of hybrid recurrent architectures, Soma (2024) showed that combining different recurrent models enhanced learning capability for sequential data analysis. Furthermore, Dintakurthy *et al.* (2025) discussed the growing role of artificial intelligence in enabling real-time and low-latency intelligent systems. Inspired by these advancements, the present work adopted an LSTM-based deep learning framework to model temporal dependencies in OFDM signals for effective ICI cancellation.

3. Proposed methodology

In our proposed framework, the received OFDM signal is first transformed from the time domain to the frequency domain using the fast Fourier transform. The resulting

complex subcarrier symbols, represented by their in-phase (I) and quadrature (Q) components, are used as input features for the LSTM network. These features are arranged as sequential vectors across consecutive OFDM symbols, enabling the LSTM model to learn temporal ICI patterns and perform accurate interference estimation. A type of neural network was developed by building on shallow neural networks with a deeper network structure. To improve the characterization of system performance, deep learning can better suit the input and output characteristics. This section presents a neural network model for ICI cancellation in an OFDM system. The MSR and MCVT models are used to construct the input sequence. The LSTM network receives the sequence.

3.1. Long short-term memory network

An LSTM is designed to stop the neural network output for a particular input from either deteriorating or blowing up as it cycles through the feedback loops. Recurrent networks outperform other neural networks in pattern recognition because of their feedback loops. Sequence learning tasks require recalling previous inputs, and LSTM networks outperform other recurrent neural network designs by addressing the so-called vanishing gradient problem. Many sequence-learning problems can be solved with LSTMs because they can learn long-term dependencies.

The linear units that make up the LSTM architecture have a self-connection and a fixed weight of 1.0. This makes it possible to preserve and then recover a value (forward pass) or gradient (backward pass) that flows into this self-recurrent unit at the appropriate time step. The output or error of the previous time step is the same as the output for the subsequent time step when the unit multiplier is used. The memory cell, a self-recurrent unit, has the capacity to retain data that are hundreds of time steps in the past. This is effective for a variety of jobs.

The goal of an LSTM, or an augmented attention-based LSTM, in the context of ICI cancellation in OFDM systems, is to efficiently model and forecast the behavior of ICI. This facilitates the use of adaptive techniques to reduce ICI and enhance system performance. Because LSTMs are built to recognize patterns in sequential data, they can be used to model the temporal dependencies arising from frequency offsets and fading channels. The LSTM examines the temporal relationships of ICI across subcarriers over multiple time steps in the input signal. An anticipated ICI value for the specified SNR is the LSTM's output. To reduce the effect of ICI, adaptive modulation and encoding techniques are guided by this prediction.

In certain cases, we would like to discard information that is in the memory cell, or cell state, and replace it with

more recent, pertinent information. However, we do not want to release extraneous information into the network, as this might confuse the rest of the recurrent net. A forget gate in the LSTM unit addresses this issue by erasing the data in the self-recurrent unit to create space for a fresh memory. To prevent any misunderstanding, it accomplishes this without releasing the information into the network. The forget gate does this by multiplying the memory cell's value by a value ranging from 0 (delete) to 1 (keep everything). The LSTM unit output from the previous time step and the current input determine the precise value. At other times, a value that must be maintained across a large number of time steps is stored in the memory cell. The LSTM model does this by including an additional gate, known as the input or write gate, which can be closed to prevent new data from entering the memory cell. In this manner, the information stored in the memory cell is safeguarded until it is required. By multiplying the memory cell's output by a value between 0 (no outputs) and 1 (preserve output), another gate modifies the memory cell's output (Figure 1). If there is competition between several memories, this output gate could be helpful. In this work, an attention mechanism was designed for the LSTM network to selectively focus on the most relevant parts of the input sequence at each time step.

3.2. Mirror symbol repetition–long short-term memory

Most of the signals received at the subcarriers are affected by ICI. MSR is one of the ICI self-cancellation techniques used in many scenarios to reduce ICC in communication systems. In this model, an LSTM network is used on MSR to improve ICI cancellation. The LSTM network effectively manages the signal and input sequence. Usually, ICI arises from carrier frequency offset, Doppler shifts, and other factors. The use of MSR improves ICI robustness through its multiple symbol-rate processing. Even with different symbol speeds, LSTMs can learn the connection between transmitted symbols and interference patterns for ICI cancellation. The proposed MSR–LSTM process is shown in Figure 2.

The input signal is pre-processed using multiple symbol rates. The signals operate at various symbol rates, producing good signals and forming a communication sequence. The generated signals are fed to the LSTM network, which performs ICI cancellation. The signal is further enhanced by performing quadrature phase-shift keying (QPSK) and binary phase-shift keying (BPSK) modulation. The enhanced interference-canceled signal is achieved at the output.

3.3. Multi-carrier vector transmission –long short-term memory

An MCVT involves transmitting data using multiple carriers as vectors rather than treating each carrier independently. This joint processing can help mitigate ICI effects. By grouping carriers into vectors, the system processes them collectively, thereby exploiting correlations between carriers. This approach helps in ICI cancellation by using advanced detection algorithms, such as vector equalization and joint demodulation, to reduce interference effects caused by frequency offsets or Doppler shifts. Using LSTM networks in MCVT for ICI cancellation combines robust signal processing with LSTM networks. The LSTM network models the sequential nature of received OFDM symbols.

For an input sequence, the LSTM gates are defined as:

(i) Forget gate:

$$f_t = \sigma(W_f [h_{t-1}, x_t] + b_f) \tag{1}$$

(ii) Input gate:

$$i_t = \sigma(W_i [h_{t-1}, x_t] + b_i) \tag{2}$$

(iii) Candidate cell state:

$$\check{C}_t = \tan h(W_c [h_{t-1}, x_t] + b_c) \tag{3}$$

(iv) Cell state update:

$$C_t = f_t C_{t-1} + i_t \check{C}_t \tag{4}$$

In this process, as shown in Figure 3, the input signal is processed with the MCVT system. The data are processed as vectors across all the carriers, and each vector has its own identity. These vectors are symbols from multiple subcarriers. The time-series vectors are generated and fed to the LSTM network. These multi-carriers are well handled by LSTM. The layers in LSTM identify the temporal and inter-carrier dependencies. The next layer in LSTM helps in subtracting the ICI factor from the received signals. The LSTM network is trained by using the labeled datasets of transmitted and received vectors with known ICI effects. During operation, the trained LSTM processes incoming signal vectors to estimate the ICI components. These estimates are subtracted from the received signal to recover the clean transmitted signal. Further post-processing of

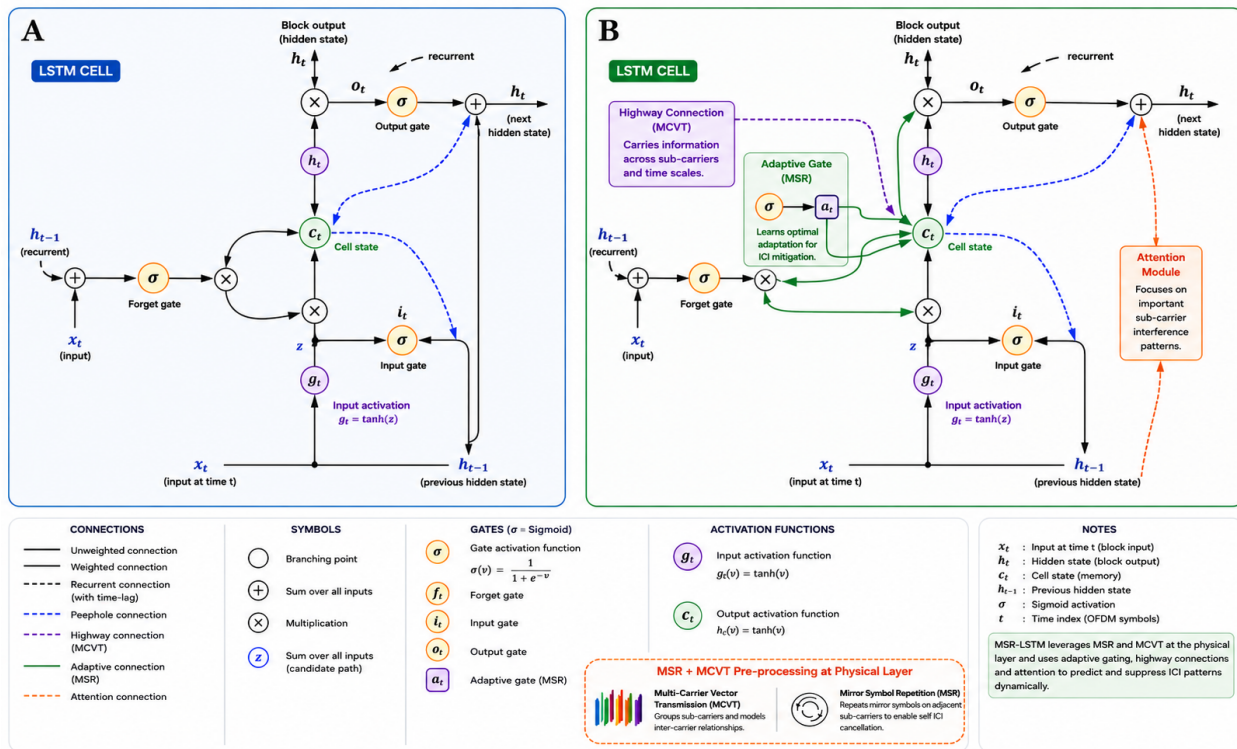


Figure 1. Architectures of (A) standard long short-term memory (LSTMs) and (B) mirror symbol repetition (MSR)-LSTM. Modified from Greff *et al.* (2017)

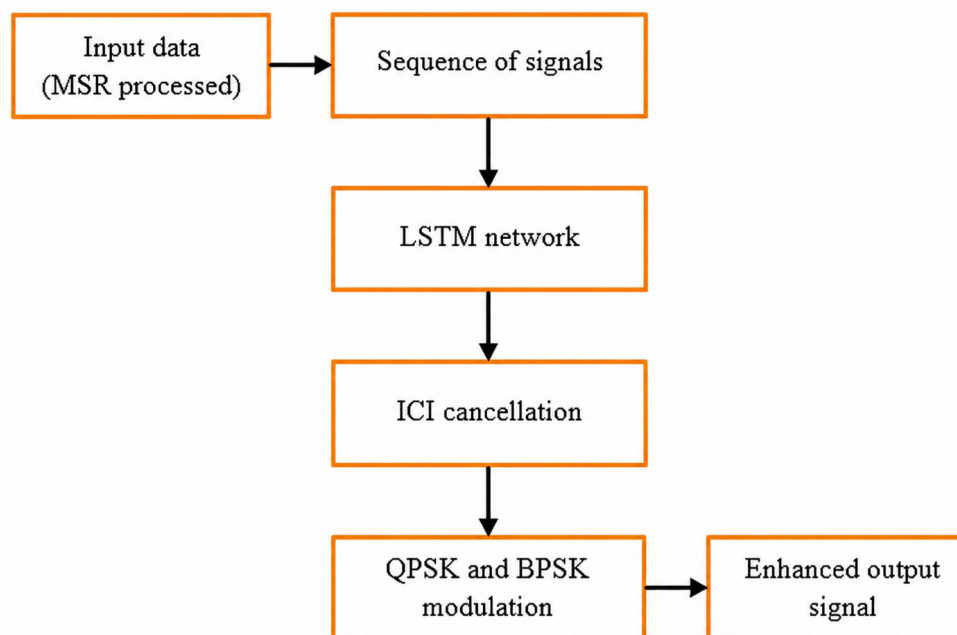


Figure 2. Process flow of the mirror symbol repetition-long short-term memory (MSR-LSTM) model
 Abbreviations: BPSK: Binary phase-shift keying; ICI: Inter-carrier interference; QPSK: Quadrature phase-shift keying.

the signal is performed using BPSK and QPSK modulation to enhance the received signal.

1.4. Modulation models

The proposed model utilizes QPSK and BPSK modulation techniques to enhance the output signal. Both techniques operate in different phases and reduce interference and BER. QPSK represents two bits per symbol using four different phase states (45°, 90°, 135°, 180°). The relatively wide Euclidean distance between symbols reduces BER in moderate noise and helps retain resilience. BPSK is the simplest form of digital modulation, as it uses only two phase states: 0° and 180°. Because the signal constellation maximizes the distance between the two symbols, it is resilient to noise. This enhances the receiver’s ability to discriminate between signals, even in the presence of interference or noise. The constellation points are maximally separated on the I–Q plane in BPSK, and binary data mapping is performed. Bit “1” is typically mapped to +1 (0° phase) and bit “0” is typically mapped to -1 (180° phase).

A BPSK-modulated signal can be represented as:

$$s(t) = A \cos^2 \left(p^i f_c t + n \right) p_i b \tag{5}$$

where A is the amplitude, f_c is the carrier frequency, and n is the binary digit (0 or 1). In the OFDM context, each subcarrier can be independently BPSK modulated.

4. Results and discussion

The OFDM with 512 subcarriers was examined in this study. One data symbol and two pilots made up each OFDM packet. Each symbol contained eight bits per subcarrier, and the QPSK and BPSK modulations were taken into consideration. The OFDM packet was sent over the Rayleigh channel after the inverse discrete Fourier transform (IDFT), with a cyclic prefix (CP) added as a guard interval to prevent inter-symbol interference. The multiuser with noise sent the OFDM packet to the media of the receiver. The LSTM network was connected, and training was performed on the signal to improve its quality.

The methodology in the work was designed on an Intel i7 processor with 32 GB of RAM, a 1 TB hard disk, and the Windows operating system. The software tool and the language model utilized were MATLAB 2024 (MathWorks, United States), with internal toolboxes such as DNN and Signal. The experimental environment is shown in Table 1.

The metrics used to evaluate the performance of the proposed MSR-LTSM and MCVT-LTSM OFDM systems were BER and CIR. These metrics were compared with

existing techniques such as the uncentered Kalman filter and the optimized uncentered Kalman filter. The MATLAB simulation was performed using the parameters stated in Table 1.

4.1. Bit error rate analysis in the additive white Gaussian noise channel

In OFDM, BER is often analyzed on an individual subcarrier basis, as each subcarrier experiences different channel conditions (e.g., fading and interference). The overall BER is an average across all subcarriers. Analytical expressions for BER depend on the modulation scheme and channel model:

$$BER_{Qpsk} = Q(x) \left(\sqrt{SNR} \right) \tag{6}$$

$$BER_{bpsk} = Q(x) \left(2 \cdot \sqrt{SNR} \right) \tag{7}$$

Here, the $Q(x)$ function is given in Equation 8:

$$Q(x) = \frac{1}{\sqrt{2\pi}} \int_x^\infty e^{-\frac{t^2}{2}} dt \tag{8}$$

The SNR is given in Equation 9.

$$SNR = \sqrt{\frac{E_s}{N_o}} \tag{9}$$

where E_s is the energy symbol and N_o is the noise power spectral. BER decreases as SNR increases, but depends on the modulation scheme.

The BER comparison for QPSK modulation using different methods is shown in Figure 4.

The BER values at different dB levels, including 0, 2, 4, 6, 8, 10, 12, 14, 16, 18, and 20, are shown in Tables 2–7. The values obtained using QPSK modulation at ep = 0 are shown in Table 2, ep = 0.3 in Table 3, and ep = 0.45 in Table 4, while those obtained using BPSK modulation at ep = 0 are shown in Table 5, ep = 0.3 in Table 6, and ep = 0.45 in Table 7.

The BER comparison for BPSK modulation using different methods is shown in Figure 5.

The performance of the system was improved with the LSTM model across all cases. Compared to modulation techniques, BPSK achieved better results than QPSK.

In the MCVT scheme, neighboring subcarriers were grouped into vectors before applying the LSTM-based interference estimation. In this work, a vector length of 8 subcarriers was used. This value was selected such

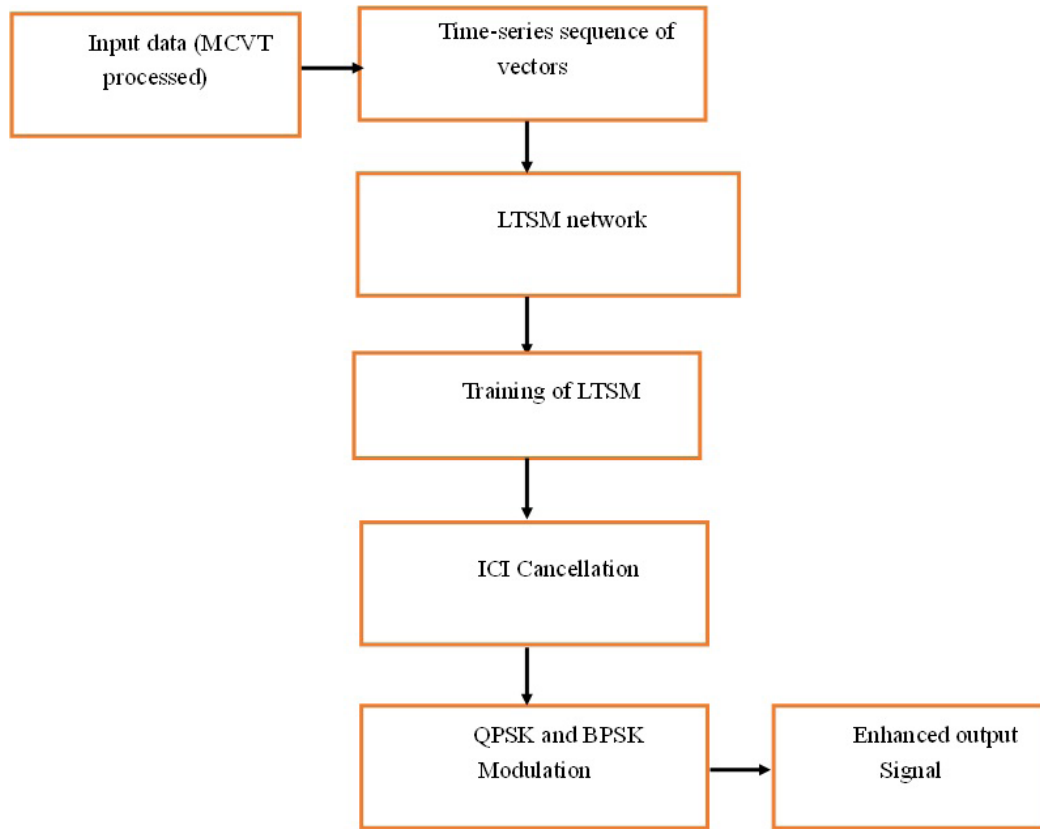


Figure 3. Process flow of the multi-carrier vector transmission–long short-term memory (MCVT–LTSM) model
 Abbreviations: BPSK: Binary phase-shift keying; ICI: Inter-carrier interference; QPSK: Quadrature phase-shift keying.

Table 1. Experimental environment

Parameter	Specification
Utilization of bits	1024
Signal-enhancing techniques	QPSK and BPSK
Type of channel noise	AWGN channel
Type of channel	Multipath channel
Deep network	LSTM
ICI cancellation model	MSR and MCVT
Size of FFT	64
Guard length	12
Size of subcarrier	512
Doppler shift	0, 0.3, 0.45
Parameters evaluated	BER and CIR

Abbreviations: AWGN: Additive white Gaussian noise; BER: Bit error rate; BPSK: Binary phase-shift keying; CIR: Carrier-to-interference ratio; FFT: Fast Fourier transform; ICI: Inter-carrier interference; LSTM: Long short-term memory; MCVT: Multi-carrier vector transmission; MSR: Mirror symbol repetition; QPSK: Quadrature phase-shift keying.

that the grouped subcarriers fall within the coherence bandwidth of the Rayleigh fading channel, ensuring that they experience approximately similar channel gains. This assumption allows the proposed model to effectively exploit the correlation among adjacent subcarriers to improve interference mitigation.

4.2. Carrier-to-interference ratio analysis in additive white Gaussian noise

The CIR is a measure of the extent to which the intended signal is affected by interference from other subcarriers in the OFDM system, typically expressed as a power ratio. In an OFDM system operating over an additive white Gaussian noise (AWGN) channel, the power level of the desired carrier signal relative to the power of interfering signals caused by ICI, which primarily arises from carrier frequency offsets, can significantly degrade system performance.

To achieve reliable communication, a minimum CIR threshold is needed. For QPSK and BPSK, this threshold is

typically lower than for higher-order modulation schemes, as they are more robust to interference. By optimizing CIR through careful design and signal processing techniques, OFDM systems can achieve robust communication even in interference-prone environments. The sole distinction between the two modulation schemes is that BPSK requires a lower CIR for reliable performance due to its simplicity and robustness, whereas QPSK requires a larger CIR for equal BER because of its denser constellation, making both systems more prone to interference. The CIR is given by Equation 10:

$$CIR = \frac{P_c}{P_i} \tag{10}$$

where P_c is the power of the derived carrier, and P_i is the total power of all the interferences. The evaluation results obtained with the proposed model using QPSK modulation are shown in Figure 6.

The results obtained by considering BPSK modulation to enhance the signal in an OFDM system are shown in Figure 7. The values of CIR with respect to various frequency offsets obtained using QPSK modulation are shown in Table 8.

The CIRs for the offset frequency in OFDM with BPSK modulation are shown in Table 9. The CIR value at 0 offset frequency was 288 dB using MCVT-LSTM. This model performed well across all offset frequencies.

In an OFDM system, a high CIR is typically preferable, as it indicates that the interference power is much weaker than that of the intended carrier signal.

4.3. Computational complexity and latency analysis

The proposed ICI cancellation model integrates ICI self-cancellation techniques with an LSTM network to improve signal quality in OFDM systems. The computational complexity of the LSTM network mainly arises from matrix multiplications in the input, forget, and output gates, as well as in the memory cell updates. For an LSTM layer with N hidden units and input sequence length T , the computational complexity is primarily due to recurrent weight operations, as follows:

$$\text{Computational complexity} = O(T \times N^2) \tag{11}$$

Although the proposed deep learning model introduces additional computational overhead compared to conventional signal processing techniques, most operations are parallelizable and can be efficiently executed using modern hardware, such as GPUs. Furthermore, the training phase is performed offline, while the inference phase used during real-time communication involves only forward propagation through the trained network, resulting in manageable latency. Therefore, the proposed MSR-LSTM and MCVT-LSTM models achieve improved interference mitigation performance while maintaining acceptable computational complexity and latency for practical OFDM communication systems.

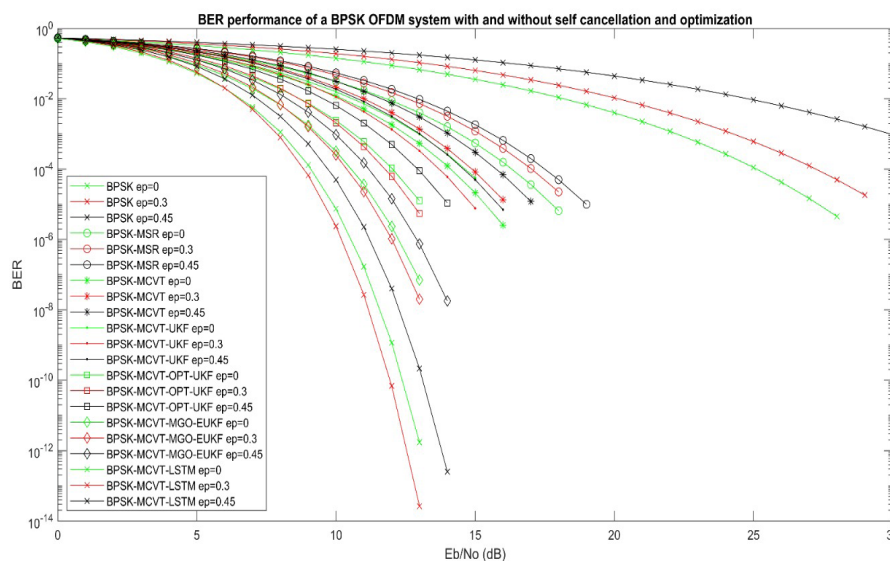


Figure 4. Bit error rate (BER) performance with respect to signal-to-noise ratio using a quadrature phase-shift keying (QPSK) modulation. Abbreviations: ep: Error probability; EUKF: Enhanced unscented Kalman filter; LSTM: Long short-term memory; MCVT: Multi-carrier vector transmission; MGO: Modified Gorilla optimization; MSR: Mirror symbol repetition; OPT: Optimized; UKF: Uncentered Kalman filter.

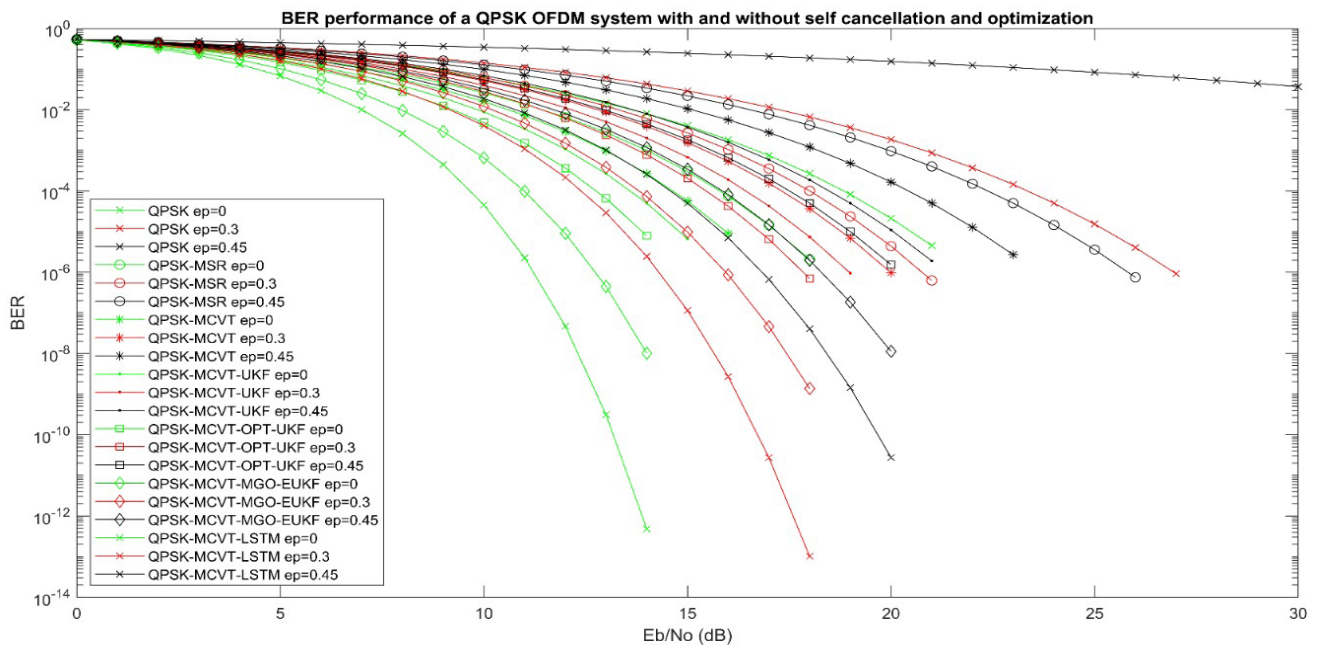


Figure 5. Bit error rate (BER) performance with respect to signal-to-noise ratio using a binary phase-shift keying (BPSK) modulation. Abbreviations: ep: Error probability; EUKF: Enhanced unscented Kalman filter; LSTM: Long short-term memory; MCVT: Multi-carrier vector transmission; MGO: Modified Gorilla optimization; MSR: Mirror symbol repetition; OPT: Optimized; UKF: Uncentered Kalman filter.

Table 2. BERs for different SNR using QPSK modulation for ep = 0

Method	SNR (dB)									
	2	4	6	8	10	12	14	16	18	20
QPSK	0.4700	0.3600	0.2500	0.1600	0.0800	0.0400	0.0140	0.0040	0.0007	0.0001
MSR	0.4600	0.3300	0.2100	0.1100	0.0450	0.0137	0.0027	0.0003	0	0
MCVT	0.4550	0.3200	0.1880	0.0884	0.0307	0.0072	0.0010	0.0001	0	0
MCVT-UKF	0.4500	0.3070	0.1661	0.0687	0.0196	0.0034	0.0003	0	0	0
MCVT-OPT-UKF	0.4460	0.2880	0.1469	0.0534	0.0124	0.0015	0.0001	0	0	0
MCVT-MGO-EUKF	0.4330	0.2510	0.1020	0.0250	0.0029	0.0001	0	0	0	0
MCVT-LSTM	0.4220	0.2160	0.0677	0.0101	0.0004	0	0	0	0	0

Abbreviations: BER: Bit error rate; ep: Error probability; EUKF: Enhanced unscented Kalman filter; LSTM: Long short-term memory; MCVT: Multi-carrier vector transmission; MGO: Modified Gorilla optimization; MSR: Mirror symbol repetition; OPT: Optimized; QPSK: Quadrature phase-shift keying; SNR: Signal-to-noise ratio; UKF: Uncentered Kalman filter.

Table 3. BER for different SNR using QPSK modulation for ep = 0.3

Method	SNR (dB)									
	2	4	6	8	10	12	14	16	18	20
QPSK	0.5003	0.4201	0.3361	0.2527	0.1750	0.1100	0.0609	0.0290	0.0114	0.0036
MSR	0.4887	0.3829	0.2737	0.1720	0.0915	0.0380	0.0123	0.0027	0.0004	0
MCVT	0.4867	0.3760	0.2630	0.1599	0.0801	0.0310	0.0080	0.0016	0.0002	0
MCVT-UKF	0.4840	0.3670	0.2480	0.1430	0.0655	0.0220	0.0050	0.0007	0	0
MCVT-OPT-UKF	0.4800	0.3560	0.2310	0.1230	0.0490	0.0140	0.0024	0.0002	0	0
MCVT-MGO-EUKF	0.4730	0.3330	0.1960	0.0876	0.0265	0.0047	0.0004	0	0	0
MCVT-LSTM	0.4660	0.3088	0.1608	0.0570	0.0118	0.0011	0	0	0	0

Abbreviations: BER: Bit error rate; ep: Error probability; EUKF: Enhanced unscented Kalman filter; LSTM: Long short-term memory; MCVT: Multi-carrier vector transmission; MGO: Modified Gorilla optimization; MSR: Mirror symbol repetition; OPT: Optimized; QPSK: Quadrature phase-shift keying; SNR: Signal-to-noise ratio; UKF: Uncentered Kalman filter.

Table 4. BER for different SNR using QPSK modulation for ep = 0.45

Method	SNR (dB)									
	2	4	6	8	10	12	14	16	18	20
QPSK	0.5200	0.4830	0.4440	0.4050	0.3640	0.3240	0.2840	0.2440	0.2067	0.1710
MSR	0.4980	0.4140	0.3260	0.2400	0.1610	0.0970	0.0502	0.0219	0.0070	0.0021
MCVT	0.4940	0.4020	0.3060	0.2130	0.1320	0.0700	0.0307	0.0106	0.0027	0.0005
MCVT-UKF	0.4900	0.3870	0.2810	0.1810	0.0990	0.0446	0.0153	0.0037	0.0006	0
MCVT-OPT-UKF	0.4870	0.3780	0.2660	0.1635	0.0833	0.0332	0.0096	0.0018	0.0002	0
MCVT-MGO-EUKF	0.4810	0.3610	0.2380	0.1310	0.0560	0.0170	0.0033	0.0003	0	0
MCVT-LSTM	0.4770	0.3445	0.2130	0.1044	0.0370	0.0083	0.0010	0	0	0

Abbreviations: BER: Bit error rate; ep: Error probability; EUKF: Enhanced unscented Kalman filter; LSTM: Long short-term memory; MCVT: Multi-carrier vector transmission; MGO: Modified Gorilla optimization; MSR: Mirror symbol repetition; OPT: Optimized; QPSK: Quadrature phase-shift keying; SNR: Signal-to-noise ratio; UKF: Uncentered Kalman filter.

Table 5. BER for different SNR using BPSK modulation for ep = 0

Method	SNR (dB)									
	2	4	6	8	10	12	14	16	18	20
BPSK	0.4830	0.4050	0.3240	0.2460	0.1740	0.1130	0.0670	0.0360	0.0168	0.0067
MSR	0.4630	0.3390	0.2190	0.1190	0.0520	0.0279	0.0040	0.0006	0	0
MCVT	0.4530	0.3120	0.1770	0.0785	0.0249	0.0100	0.0005	0	0	0
MCVT-UKF	0.4560	0.3190	0.1880	0.0884	0.0307	0.0043	0	0	0	0
MCVT-OPT-UKF	0.4410	0.2740	0.1290	0.0408	0.0075	0.0004	0	0	0	0
MCVT-MGO-EUKF	0.4290	0.2410	0.0190	0.0018	0	0	0	0	0	0
MCVT-LSTM	0.4150	0.1980	0.0530	0.006	0.0001	0	0	0	0	0

Abbreviations: BER: Bit error rate; BPSK: Binary phase-shift keying; ep: Error probability; EUKF: Enhanced unscented Kalman filter; LSTM: Long short-term memory; MCVT: Multi-carrier vector transmission; MGO: Modified Gorilla optimization; MSR: Mirror symbol repetition; OPT: Optimized; SNR: Signal-to-noise ratio; UKF: Uncentered Kalman filter.

Table 6. BER for different SNR using BPSK modulation for ep = 0.3

Method	SNR (dB)									
	2	4	6	8	10	12	14	16	18	20
BPSK	0.5060	0.4370	0.3660	0.2940	0.2240	0.1600	0.1060	0.0640	0.0345	0.0163
MSR	0.4850	0.3370	0.2580	0.1540	0.0752	0.0279	0.0073	0.0012	0.0001	0
MCVT	0.4780	0.3480	0.2190	0.1110	0.0411	0.0100	0.0014	0.0001	0	0
MCVT-UKF	0.4730	0.3310	0.1930	0.0850	0.0253	0.0043	0.0003	0	0	0
MCVT-OPT-UKF	0.4620	0.2960	0.1440	0.0450	0.0072	0.0003	0	0	0	0
MCVT-MGO-EUKF	0.4510	0.2640	0.1040	0.0210	0.0016	0	0	0	0	0
MCVT-LSTM	0.4350	0.2160	0.0570	0	0	0	0	0	0	0

Abbreviations: BER: Bit error rate; BPSK: Binary phase-shift keying; ep: Error probability; EUKF: Enhanced unscented Kalman filter; LSTM: Long short-term memory; MCVT: Multi-carrier vector transmission; MGO: Modified Gorilla optimization; MSR: Mirror symbol repetition; OPT: Optimized; SNR: Signal-to-noise ratio; UKF: Uncentered Kalman filter.

Table 7. BER for different SNR using BPSK modulation for ep = 0.45

Method	SNR (dB)									
	2	4	6	8	10	12	14	16	18	20
QPSK	0.5120	0.4570	0.4000	0.3410	0.2830	0.2260	0.1740	0.1270	0.0877	0.0567
MSR	0.4870	0.3780	0.2660	0.1630	0.0830	0.0330	0.0096	0.0020	0.0002	0
MCVT	0.4820	0.3590	0.2360	0.1290	0.0540	0.0160	0.0031	0.2300	0	0
MCVT-UKF	0.4770	0.3440	0.2130	0.1040	0.0370	0.0080	0.0010	0	0	0
MCVT-OPT-UKF	0.4680	0.3190	0.1750	0.0680	0.0167	0.0020	0	0	0	0
MCVT-MGO-EUKF	0.4570	0.2830	0.1270	0.0340	0.0040	0	0	0	0	0
MCVT-LSTM	0.4440	0.2450	0.0830	0.0130	0.0005	0	0	0	0	0

Abbreviations: BER: Bit error rate; BPSK: Binary phase-shift keying; ep: Error probability; EUKF: Enhanced unscented Kalman filter; LSTM: Long short-term memory; MCVT: Multi-carrier vector transmission; MGO: Modified Gorilla optimization; MSR: Mirror symbol repetition; OPT: Optimized; SNR: Signal-to-noise ratio; UKF: Uncentered Kalman filter.

Table 8. CIR values with a QPSK-modulated OFDM system

Method	Offset frequency (kHz)								
	0.05	0.10	0.15	0.20	0.25	0.30	0.35	0.40	0.45
QPSK	55.00	33.36	20.23	12.27	7.44	4.51	2.74	1.66	1.01
Q-MSR	70.00	47.99	34.78	26.86	22.12	19.27	17.56	16.53	15.92
Q-MCVT	80.00	55.59	41.11	32.52	27.43	24.41	22.61	21.55	20.92
Q-MCVT-UKF	115.00	83.99	65.81	55.14	48.88	45.21	43.05	51.79	41.05
Q-MCVT-OPT-UKF	200.00	158.00	133.65	119.50	111.30	106.50	103.80	102.20	101.20
Q-MCVT-MGO-EUKF	250.00	198.80	169.50	152.60	143.00	137.50	134.30	132.50	131.40
Q-MCVT-LSTM	265.00	213.80	184.40	167.60	158.00	152.50	149.30	147.50	146.40

Abbreviations: EUKF: Enhanced unscented Kalman filter; LSTM: Long short-term memory; MCVT: Multi-carrier vector transmission; MGO: Modified Gorilla optimization; MSR: Mirror symbol repetition; OFDM: Orthogonal frequency division multiplexing; OPT: Optimized; QPSK: Quadrature phase-shift keying; UKF: Uncentered Kalman filter.

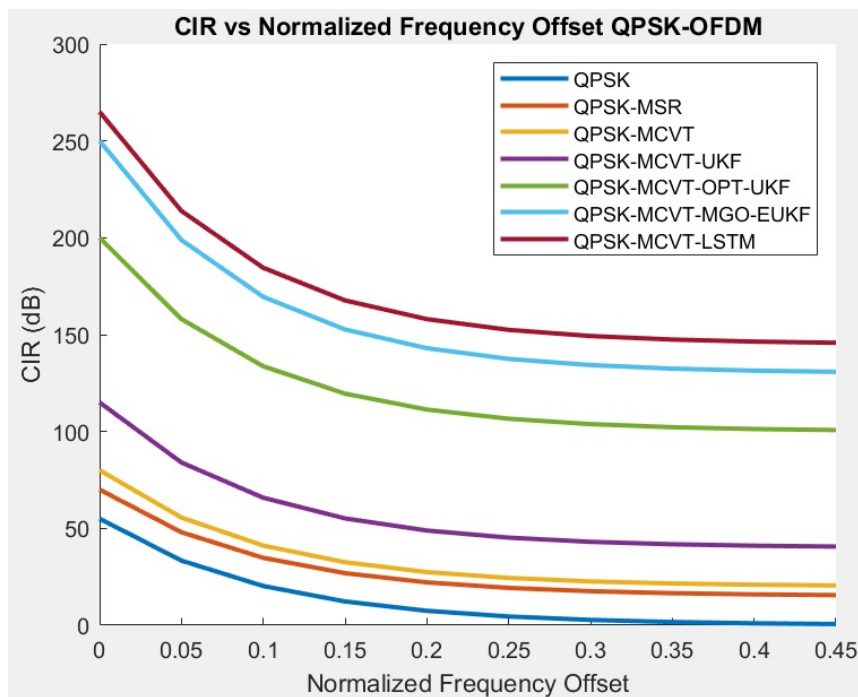


Figure 6. Performance of CIR using QPSK modulation

Abbreviations: CIR: Carrier-to-interference ratio; EUKF: Enhanced unscented Kalman filter; LSTM: Long short-term memory; MCVT: Multi-carrier vector transmission; MGO: Modified Gorilla optimization; MSR: Mirror symbol repetition; OFDM: Orthogonal frequency division multiplexing; OPT: Optimized; QPSK: Quadrature phase-shift keying; UKF: Uncentered Kalman filter.

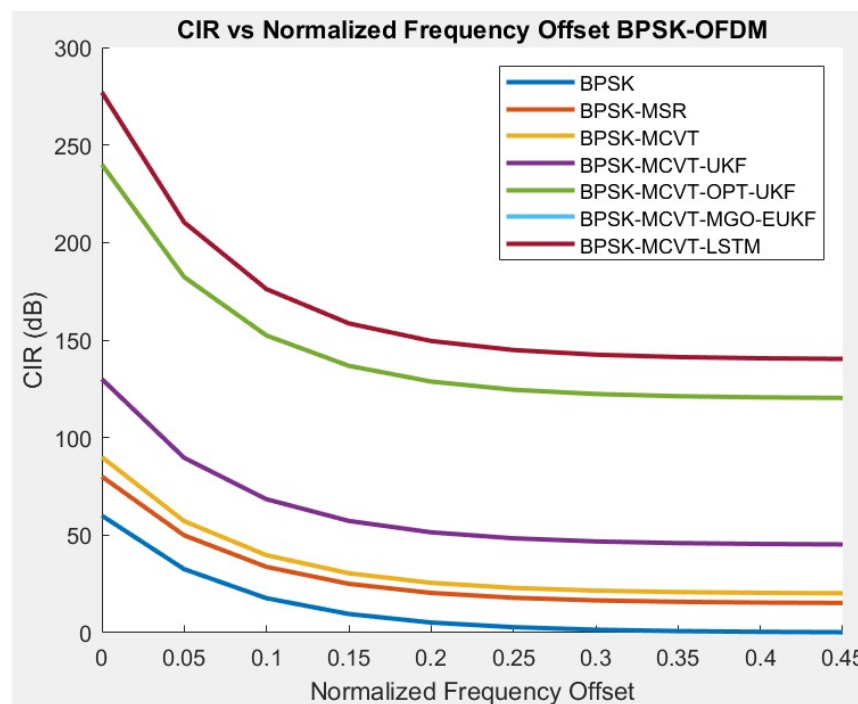


Figure 7. Performance of CIR using BPSK modulation

Abbreviations: BPSK: Binary phase-shift keying; CIR: Carrier-to-interference ratio; EUKF: Enhanced unscented Kalman filter; LSTM: Long short-term memory; MCVT: Multi-carrier vector transmission; MGO: Modified Gorilla optimization; MSR: Mirror symbol repetition; OFDM: Orthogonal frequency division multiplexing; OPT: Optimized; UKF: Uncentered Kalman filter.

Table 9. CIR values with a BPSK-modulated OFDM system

Method	Offset frequency (kHz)								
	0.05	0.10	0.15	0.20	0.25	0.30	0.35	0.40	0.45
QPSK	60.00	32.56	17.67	9.59	5.21	2.83	1.53	0.83	0.45
Q-MSR	80.00	49.80	33.70	25.05	20.39	17.89	16.55	15.83	15.44
Q-MCVT	90.00	57.15	39.72	30.47	25.55	22.95	21.56	20.83	20.44
Q-MCVT-UKF	130.00	89.62	68.42	57.29	51.45	48.38	46.77	45.93	45.49
Q-MCVT-OPT-UKF	240.00	182.20	152.30	136.79	128.71	124.52	122.30	121.20	120.60
Q-MCVT-MGO-EUKF	277.00	210.30	176.10	158.50	149.50	144.80	142.50	141.20	140.60
Q-MCVT-LSTM	288.00	216.50	182.50	170.20	156.10	150.00	148.20	145.10	143.40

Abbreviations: BPSK: Binary phase-shift keying; EUKF: Enhanced unscented Kalman filter; LSTM: Long short-term memory; MCVT: Multi-carrier vector transmission; MGO: Modified Gorilla optimization; MSR: Mirror symbol repetition; OFDM: Orthogonal frequency division multiplexing; OPT: Optimized; UKF: Uncentered Kalman filter.

5. Conclusion

The work aims to improve the performance of the OFDM system by eliminating ICI and enhancing signal quality. The experimental results were evaluated using deep learning and ICI self-cancellation techniques. The input signal was crafted using MSR and MCVT techniques, and the processing was done using an LSTM network. Although LSTMs were designed to model sequences, they treated all inputs equally, leading to suboptimal performance. To improve prediction accuracy and interpretability, this research introduces an attention mechanism into the LSTM that dynamically focuses on the most relevant parts of the sequence. Attention-enhanced LSTMs offer a major improvement over conventional LSTMs for both general and specific applications, such as ICI cancellation, particularly when handling noisy or lengthy sequential inputs. The results show notable gains in key performance indicators, including lower BER and higher CIR. Overall, the recommended deep learning-based ICI approaches demonstrated robust and reliable performance across a range of Doppler shifts, including 0, 0.30, and 0.45 kHz, effectively maintaining a low bit error rate without introducing excessive computational overhead.

Acknowledgments

None.

Funding

None.

Conflict of interest

The authors declare they have no competing interests.

Author contributions

Conceptualization: Sailakshmi Kumari Narava, Kavi Priya Periasami

Formal analysis: Kavi Priya Periasami

Investigation: Sailakshmi Kumari Narava

Methodology: Sailakshmi Kumari Narava

Supervision: Kavi Priya Periasami

Visualization: Sailakshmi Kumari Narava, Kavi Priya Periasami

Writing-original draft: Sailakshmi Kumari Narava

Writing-review & editing: Sailakshmi Kumari Narava, Kavi Priya Periasami

Availability of data

The data are available from the corresponding author upon reasonable request.

References

- Bai, S., Kilby, J., & Prasad, K. (2026). Deep Learning-Based Channel Estimation Techniques Using IEEE 802.11p Protocol, Limitations of IEEE 802.11p and Future Directions of IEEE 802.11bd: A Review. *Sensors*, 26(5), 1658. <https://doi.org/10.3390/s26051658>
- Basholli, F., Hayal, M. R., Elsayed, E. E., & Juraev, D. A. (2025). Deep Learning for Skin Disease Classification: A Comparative Study of CNN and CNN-LSTM Architectures. *Journal of Computing and Data Technology*, 1(1), 40–49. <https://doi.org/10.71426/jcdt.v1.i1.pp40-49>
- Bazzi, A., Slock, D. T. M., & Meilhac, L. (2015). Efficient Maximum Likelihood Joint Estimation of Angles and Times of Arrival of Multiple Paths. In: *2015 IEEE GlobeCom Workshops (GC Workshops)* (pp. 1–7). IEEE. 2015 IEEE GlobeCom Workshops (GC Workshops). <https://doi.org/10.1109/glocomw.2015.7414203>
- Dintakurthy, Y., Innmuri, R. K., Vanteru, A., & Thotakuri, A. (2025). Emerging Applications of Artificial Intelligence in Edge Computing: A Comprehensive Review. *Journal of Modern Technology*, 175–185. <https://doi.org/10.71426/jmt.v1.i2.pp175-185>

- Essai Ali, M. H. (2020). Deep learning-based pilot-assisted channel state estimator for OFDM systems. *IET Communications*, 15(2), 257–264.
<https://doi.org/10.1049/cmu2.12051>
- Greff, K., Srivastava, R. K., Koutnik, J., Steunebrink, B. R., & Schmidhuber, J. (2017). LSTM: A Search Space Odyssey. *IEEE Transactions on Neural Networks and Learning Systems*, 28(10), 2222–2232.
<https://doi.org/10.1109/tnnls.2016.2582924>
- Huang, H., Guo, S., Gui, G., Yang, Z., Zhang, J., Sari, H., & Adachi, F. (2020). Deep Learning for Physical-Layer 5G Wireless Techniques: Opportunities, Challenges and Solutions. *IEEE Wireless Communications*, 27(1), 214–222.
<https://doi.org/10.1109/mwc.2019.1900027>
- Jdid, B., Hassan, K., Dayoub, I., Lim, W. H., & Mokayef, M. (2021). Machine Learning Based Automatic Modulation Recognition for Wireless Communications: A Comprehensive Survey. *IEEE Access*, 9, 57851–57873.
<https://doi.org/10.1109/access.2021.3071801>
- Krishnama Raju, A., Gupta, S., & Jaiswal, A. (2022). An Efficient Deep Neural Networks-Based Channel Estimation and Signal Detection in OFDM Systems. In: *Lecture Notes in Networks and Systems* (pp. 603–613). Springer Nature Singapore.
https://doi.org/10.1007/978-981-16-6246-1_51
- Khan, I., Zafar, M. H., Ashraf, M., & Kim, S. (2018). Computationally Efficient Channel Estimation in 5G Massive Multiple-Input Multiple-output Systems. *Electronics*, 7(12), 382.
<https://doi.org/10.3390/electronics7120382>
- Le, H. A., Van Chien, T., Nguyen, T. H., Choo, H., & Nguyen, V. D. (2021). Machine Learning-Based 5G-and-Beyond Channel Estimation for MIMO-OFDM Communication Systems. *Sensors*, 21(14), 4861.
<https://doi.org/10.3390/s21144861>
- Li, L., Chen, H., Chang, H. H., & Liu, L. (2020). Deep Residual Learning Meets OFDM Channel Estimation. *IEEE Wireless Communications Letters*, 9(5), 615–618.
<https://doi.org/10.1109/lwc.2019.2962796>
- Logins, A., He, J., & Paramonov, K. (2022). Block-Structured Deep Learning-Based OFDM Channel Equalization. *IEEE Communications Letters*, 26(2), 321–324.
<https://doi.org/10.1109/lcomm.2021.3133018>
- Ly, A., & Yao, Y. D. (2021). A Review of Deep Learning in 5G Research: Channel Coding, Massive MIMO, Multiple Access, Resource Allocation, and Network Security. *IEEE Open Journal of the Communications Society*, 2, 396–408.
<https://doi.org/10.1109/ojcoms.2021.3058353>
- Mei, K., Liu, J., Zhang, X., Cao, K., Rajatheva, N., & Wei, J. (2021). A Low Complexity Learning-Based Channel Estimation for OFDM Systems With Online Training. *IEEE Transactions on Communications*, 69(10), 6722–6733.
<https://doi.org/10.1109/tcomm.2021.3095198>
- Miao, P., Chen, G., Cumanan, K., Yao, Y., & Chambers, J. A. (2022). Deep Hybrid Neural Network-Based Channel Equalization in Visible Light Communication. *IEEE Communications Letters*, 26(7), 1593–1597.
<https://doi.org/10.1109/lcomm.2022.3172219>
- Mthethwa, B., & Xu, H. (2020). Deep Learning-Based Wireless Channel Estimation for MIMO Uncoded Space-Time Labeling Diversity. *IEEE Access*, 8, 224608–224620.
<https://doi.org/10.1109/access.2020.3044097>
- Nair, A. K., & Menon, V. (2022). Joint Channel Estimation and Symbol Detection in MIMO-OFDM Systems: A Deep Learning Approach using Bi-LSTM. In: *Proceedings of 2022 14th International Conference on Communication Systems & Networks (COMSNETS)* (pp. 406–411). IEEE.
<https://doi.org/10.1109/comsnets53615.2022.9668456>
- Reddy, S. R. S., Akshaya, G. N., Koteswari, O. L., Sreeja, T., & Edara, V. S. (2025). Leveraging Sentiment Analysis in the Digital Era: Uncovering Insights from Unstructured Data for Enhanced Customer Engagement. *Journal of Modern Technology*, 02(01), 212–219.
<https://doi.org/10.71426/jmt.v2.i1.pp212-219>
- Shamasundar, B., & Chockalingam, A. (2019). A DNN Architecture for the Detection of Generalized Spatial Modulation Signals (Version 2). *arXiv*.
<https://doi.org/10.48550/ARXIV.1910.01948>
- Soma, A. k. (2024). Hybrid RNN-GRU-LSTM Model for Accurate Detection of DDoS Attacks on IDS Dataset. *Journal of Modern Technology*, 2(1), 283–291.
<https://doi.org/10.71426/jmt.v2.i1.pp283-291>
- Wang, S., Yao, R., Tsiftsis, T. A., Miridakis, N. I., & Qi, N. (2020). Signal Detection in Uplink Time-Varying OFDM Systems Using RNN With Bidirectional LSTM. *IEEE Wireless Communications Letters*, 9(11), 1947–1951.
<https://doi.org/10.1109/lwc.2020.3009170>
- Ye, H., Li, G. Y., & Juang, B. H. (2018). Power of Deep Learning for Channel Estimation and Signal Detection in OFDM Systems. *IEEE Wireless Communications Letters*, 7(1), 114–117.
<https://doi.org/10.1109/lwc.2017.2757490>